CHARACTERIZATION AND MODELING OF CEMENTS FOR GEOTHERMAL WELL CASING REMEDIATION

A.J. Philippacopoulos and M.L. Berndt
Department of Energy Sciences and Technology
Brookhaven National Laboratory

(Geothermal Resources Council Transactions, Vol. 24, 81-86, San Francisco, 2000)

****

TABLE OF CONTENTS

****

ABSTRACT

A proposed strategy to remediate geothermal wells with deformed casing involves milling out the damaged section and cementing a liner in place to form a patch. Finite element models were developed to evaluate the global and local response of remediated wells to axial and shear deformation mechanisms. Different cement formulations were tested to enable property description of cements originally used in the wells and to evaluate suitability as patch materials. Compressive, tensile and flexural strengths and other material properties were measured.

INTRODUCTION

Several casings of geothermal wells have been subjected to excessive deformations resulting in loss of production. The precise nature of what causes these wells to excessively deform is currently not known. Formation movement, which in turn, is associated with the long-term response of the site due to tectonic or other loads such as those related to subsidence are suspected to be among the main causes. Deformation of well casing is also experienced in petroleum fields and attributed to subsidence and reservoir compaction (see e.g., Wagg et al., 1999; Hilbert et al., 1999; Dusseault et al., 1998 and Fredrich et al., 1996). Remediation of deformed well casing is a cost-effective alternative to plugging and abandonment. A GDO project has developed a remediation procedure to be used at The Geysers geothermal field. It involves: (a) plugging of the geothermal well temporarily using an isolation packer, (b) milling the deformed area and (c) patching the area using a steel liner which is cemented into place. Some aspects of the casing remediation program are described by Knudsen et al. (1999).

The overall objective of our research is to: (a) develop suitable cements for application to geothermal well casing remediation and (b) evaluate the strength of the remediated well casing system and determine whether cement properties can be tailored to mitigate future casing damage. Initially, a survey of well cement properties, prior casing deformation studies and the type of analysis required to recommend a patch cement was performed (Allan and Philippacopoulos, 1998).

The design and development of cement materials for casing remediation was further supported by numerical modeling studies. Two categories of analysis were considered. The first is a global analysis required to define the overall deformation mechanisms at the geothermal field that are responsible for causing casing failures. Modeling of the formation is concerned only with major property variations with depth so that key layering features of the site are represented. Emphasis, however, is placed on boundary conditions or more generally on defining the free-field loading which is responsible for the formation movement observed at the site. For global analysis we employed geomechanical finite element models that included various formation layers. The second type of analysis is a local one. It addresses the stress and deformation fields in the vicinity of the remediation area. While the global analysis is primarily concerned with the overall response of the site, i.e., shape of the failure mode, the local analysis employs a detailed numerical modeling of the casing-cement-formation interaction. For local analysis, structural finite element models were developed and used to obtain the stresses and deformations in the vicinity of the remediation. Finite element analysis was performed using the ANSYS computer program.

GEOMECHANICAL MODELS

For global analysis, finite element plane strain geomechanical models of the formation were developed. By assuming that lateral formation movements cause casing deformations, geomechanical models were run to evaluate the corresponding stress field. This was followed by structural calculations using cross-sectional and material properties of the casing. Numerical results were obtained by the following procedure: The stress field was first defined along a pre-selected interface of the plane strain model. Specifically, a uniform resultant force distribution was assumed, the magnitude of which was incrementally brought up to higher values until the material failed along the interface. Shearing was simulated using contact elements with a representative range of properties. Accordingly, the respective stress and deformation fields were evaluated. If a geothermal well penetrates this interface it is anticipated to undergo significant stresses. Using the displacements from the geomechanical model and by assuming beam type behavior, the stresses (bending and shear) at the casing were evaluated. It was found that 80-120 mm lateral displacements could result in yielding of the casing.

Primarily two layers were considered in the plane strain model to simulate a serpentinite layer overlaying the main greywacke as encountered in The Geysers geologic profile. For simplicity, horizontal layering is assumed to represent the formation (typically the site has layers dipping at about 20^{o}). The model was 3000 ft deep and 1000 ft wide. It consists of 2,652 nodes and 2,548 elements. Elastic properties of the top and bottom layers were elastic modulus, E = 0.06 GPa, Poisson's ratio, ν = 0.45 and E = 0.70 GPa, ν = 0.3, respectively. Nonlinear analysis was

performed using parametric variations due to uncertainties in property values for the contact elements. Solutions usually converged after 5 to 15 iterations. Principal stresses for lateral formation movement are shown in Figure 1. Subsequent analysis was performed by incorporating the casing at the center of the plane strain model. Two layers of elements were used for the casing and, thus, their material property (basically the Young's modulus) was treated parametrically to reasonably simulate the casing bending rigidity. Figure 2 displays the shear stress distribution which is apparently amplified around the casing and particularly near the interface between the two layers where a maximum differential displacement occurs due to the lateral sliding of the serpentinite. The deformed shape of the configuration is shown in Figure 3. The latter figure also shows a detail of the deformation pattern in the vicinity of the maximum stresses from which it can be seen that the casing has been excessively deformed due to the shearing forces exerted by the formation movement.

Currently, lack of deformation data limits the use of geomechanical models. Because of the number of assumptions that have to be made, the analysis is not well constrained. As more casing deformation data become available, however, global analysis using geomechanical models will become a more useful tool in quantitative analysis. Meanwhile, qualitative evaluations based on the location of the well and the characteristics of the formation are made. Accordingly, casing deformations are often attributed to movement of formation rocks along interfaces of high contrast in material strength. For example, interfaces involving the serpentinite, greenstone and greywacke are possible candidates. Especially, serpentinite is known to be a very soft and ductile material. Deformation field measurements confirm such possibilities. However, deformed wells were found in other areas of the field. Some of them seem to correlate with the subsidence at The Geysers especially in the northwest and southeast parts of the field. Based on Mossop et al. (1997), the site has seen maximum subsidence of about one meter since 1977. Subsidence due to reservoir compaction has also been found as the responsible mechanism for oil fields (see e.g., Fredrich et al., 1996).

STRUCTURAL MODELS

Structural models were developed to analyze the local behavior of the casing-cement-formation interaction in geothermal wells. Similarly, general lumped-parameter models in which the casing is represented by beam elements while the formation by spring elements could be also used for this purpose. In this study, however, we concentrated on detailed localized models in which both the well casing as well as the surrounding formation are modeled with solid finite elements. A schematic of a typical remediation area of a geothermal well is given in Figure 4a. The key components of the casing patch are the liner and the cemented annulus. The latter is the space between the liner and the inner well casing. The same cement can be also placed in the volume between the casing and the formation created by milling operations. The cement for the casing patch is required for redistribution of stresses due to formation loads in addition to those induced by thermal and pressure effects during production. Discontinuities due to the lack of casing are responsible for redistributing the loads in this junction thus making the cement responsible for taking on some of the local stresses.

Three-dimensional finite element models representing local behavior of geothermal wells were developed. These wells are assumed to be candidates for potential remediation using the cement

mixes described below. Our numerical study considers typical modes of casing failure, i.e., axial and shear. For a given mode, the corresponding stress and deformation fields are evaluated. A typical finite element model used in our numerical studies is shown in Figure 4b. Due to symmetry of the failure modes considered thus far, only half of the model is necessary. The model has 2,275 nodes and 1,723 three-dimensional solid elements. It incorporates following components: (a) 7" liner; (b) 13 3/8" inner casing and (c) 16" outer casing. All casing is K-55 carbon steel. The patch cement occupies the space between the 7" liner and the 13 3/8" casing as well as the area created by milling the deformed well. In addition, both casings are assumed to originally be cemented with a standard Class G cement/40%silica flour mix.

All steel parts of the models were assumed to have E = 200 GPa and ν = 0.3. Cements employed originally to complete the well were assigned the following elastic properties: E = 14 GPa and ν = 0.2. Properties of the cements for the patch construction were obtained from our experimental program described in the next section. Our analysis was particularly focused on the specific properties of the patch cement and their effect on the stress magnitudes. Material development and modeling studies are carried out interactively to optimize the properties of the proposed materials. Finally, the formation was extended up to six times the inner radius of the configuration. The well is assumed to penetrate interfaces between different layers at the site involving the serpentinite, greenstone or greywacke rocks. Some of the most severe cases measured in wellbore deformation surveys involve contrasts between the serpentinite and greywacke. Therefore, the properties of the formation assigned in the model vary from soft to harder rocks (E = 0.1 to 1.0 GPa).

By accounting for complete casing-cement-rock interaction, the three-dimensional model was employed for two types of well damage mechanisms, namely, axial and shear. These are among the basic mechanisms encountered in geothermal fields. In cases of reservoir compaction, the casing could experience buckling and collapse due to axial compression. Lack of lateral support due to cavities behind the casing amplifies the damage. Casing shear is a predominant mode of failure (Dusseault et al., 1998) and several analyses were performed using the model shown in Figure 4b. Shearing was simulated by imposing displacement boundary conditions at the model so that it resembles a beam deformed in shear mode (pure translation at both ends without end rotation). In addition, the overburden stress was applied at the end nodes assuming that the depth of remediation is 840 feet (typical for Biegel 3). Some stress contours associated with axial and shearing deformation mechanisms are shown in Figure 5. These preliminary results indicate the necessity of the patch cement to exhibit tensile capacity when subjected to shear deformations. Currently, we are conducting parametric studies that relate the axial or lateral displacement with the resulting stresses at the remediation patch for both modes of deformation.

CEMENT DESIGN AND DEVELOPMENT

Experimental Procedure

Three cement mixes were selected for initial material property determination. The properties are required in the numerical analysis component to describe cements originally used in wells and to evaluate suitability as patch materials. The baseline mix was standard Class G cement/40% silica flour with a density of 1.92 g/cm^3 (16 lb/gal.) and the variations on this were latex-

modification and partial replacement of cement with metakaolin. Work on a perlite containing mix with density of 1.68 g/cm^3 (14 lb/gal.) is in progress as this has been used at The Geysers. Preliminary studies on carbon and glass fibre reinforced cements have also been conducted. API Class G cement was provided by Mountain Cement Co. The silica flour used was 200 mesh and supplied by Halliburton Energy Services. Latex was studied for the potential to improve tensile, flexural and bonding properties. The latex was sytrene butadiene rubber supplied by BJ Services (BA-86L). A polymer solids/cement ratio of 0.10 by mass was used. Metakaolin was of interest for improving strength and for preventing strength retrogression in glass fibre reinforced cements (Marikunte et al., 1997). MetaMax® metakaolin supplied by Engelhard Corporation was used at a cement replacement level of 10% by mass. A dispersant and bentonite were added to improve pumpability and reduce bleeding, respectively. Table 1 gives the mix proportions of the slurries.

Table 1. Mix proportions of tested cements by mass.

Mix Code	Cement	Silica Flour	Metakaolin	Water	Latex	Bentonite	Dispersant	Density (g/cm^3)
40SF	1	0.4	-	0.55	-	0.034	0.012	1.92
40SFL	1	0.4	-	0.343	0.217	0.01	0.006	1.89
40SFM	0.9	0.4	0.1	0.55	-	0.015	0.012	1.90

The cements were tested for compressive, splitting tensile and flexural strengths, and dynamic and thermal properties. All specimens were cured in water for 28 days at 52^{o}C (125^{o}F). The curing temperature was selected to represent in-situ thermal conditions at a depth of 30.5 m (1000 ft) which is typical of the zone requiring remediation.

Uniaxial compressive strength tests were performed on cylinders 51 mm diameter and 102 mm long following ASTM C 39. The first series of tests was conducted at room temperature and the second at 200^{o}C (392^{o}F) is in progress. The elevated temperature represents conditions that the cement may be exposed to after remediation is completed and the well is operational. The cements are also being tested for static elastic properties and under triaxial compression at 200^{o}C

Splitting tensile strength at room temperature was measured in accordance with ASTM C 496 on cylinders 76 mm diameter and 145 mm long. Beams 51 mm by 51 mm by 305 mm were used for flexural strength tests at room temperature (ASTM C 78). The coefficient of thermal expansion was measured on beams of the same dimensions as those for the flexural strength tests following ASTM C 531. The change in linear dimension between 52 and 90^{o}C was determined. Thermal conductivity was measured using the hot wire method. Dynamic elastic properties (ASTM C 215) were measured on beams 51 mm by 51 mm by 204 mm at room temperature. The dynamic elastic modulus is sensitive to microcracking and will be used to monitor any changes in elastic properties and hence, long-term durability.

Experimental Results and Discussion

The results obtained to date are presented in Tables 2 and 3. Assuming that the strength data are normally distributed, a t-test can be used to compare the sample means. Two tailed tests at 5% level of significance were performed. This analysis showed that the metakaolin-modified

cement (40SFM) had a significantly lower mean compressive strength from the unmodified (40SF) and latex-modified (40SFL) mixes. Comparing the splitting tensile strengths indicated that the latex- and metakaolin-modified cements had significantly lower strengths than the unmodified mix. Thus, the latex did not improve indirect tensile strength under the conditions tested. However, latex did increase flexural strength. The coefficient of thermal expansion was influenced by addition of either latex or metakaolin. The latex-modified mix had a higher thermal conductivity. Comparing the dynamic properties, the only significant difference was the increase in shear modulus associated with use of metakaolin. It is expected that the static modulus of elasticity and Poisson's ratio will be lower than the dynamic values.

Table 2. Static and thermal properties of tested cements.

Mix Code	Compressive Strength (MPa)	Tensile Strength (MPa)	Flexural Strength (MPa)	Thermal Conductivity (W/m.K)	Coefficient of Thermal Expansion ($^oC^{-1}$)
40SF	38.9 ± 4.2	5.20 ±0.08	4.95 ± 0.47	0.867 ± 0.011	$9.55 \times 10^{-6} \pm 6.5 \times 10^{-7}$
40SFL	35.9 ± 3.5	4.62 ± 0.60	6.88 ± 0.56	0.954 ± 0.059	$6.98 \times 10^{-6} \pm 8.3 \times 10^{-7}$
40SFM	30.1 ± 3.4	4.95 ± 0.19	5.11 ± 0.47	0.844 ± 0.033	$1.30 \times 10^{-5} \pm 6.0 \times 10^{-7}$

Table 3. Dynamic properties of tested cements.

Mix Code	Elastic Modulus (GPa)	Shear Modulus (GPa)	Poisson's Ratio
40SF	16.7 ± 0.5	6.67 ± 0.12	0.25 ± 0.02
40SFM	17.5 ± 0.4	6.96 ± 0.07	0.25 ± 0.02
40SFL	17.4 ± 0.4	6.88 ± 0.21	0.26 ± 0.03

Strength, elastic modulii and Poisson's ratio are predicted to decrease at elevated temperature based on data obtained from Portland cement concrete (Bazant and Kaplan, 1996). The magnitude of decrease in these properties for patch and original well cements is being determined. This will be integrated with the numerical modeling studies to predict the behavior of wells repaired with different cements. Future research will examine the properties of foam, fibre reinforced and other cements to evaluate suitability for well remediation.

CONCLUSIONS

Finite element models describing geomechanical and structural aspects of well casing remediation were developed. Preliminary analysis was performed to examine the response of a remediated well configuration to axial and shear deformations. The results obtained from our numerical studies confirm the importance of the cement properties on the response of the casing patch. Strength and other properties of Class G cement/silica flour-based formulations were measured. The initial results showed that latex significantly improved flexural strength and that metakaolin did not impart any major benefits. The significance of these findings on the behavior of the patched well is under investigation. More detailed analysis, together with elevated temperature and multiaxial property determination, is in progress and will enable better understanding and prediction of cement patch requirements and performance.

ACKNOWLEDGEMENTS

This work was supported by the U.S. Department of Energy Office of Geothermal and Wind Technologies and performed under contract number DE-AC02-98CH10886. The program manager is Ray LaSala. The assistance of Ahmet Kucuk, Matthew Gold and Christopher Dambra, SUNY at Stony Brook, in performing the flexural strength tests is much appreciated.

REFERENCES

Allan, M.L. and Philippacopoulos, A.J., 1998, Literature Survey on Cements for Remediation of Deformed Casing in Geothermal Wells, BNL 66071, Brookhaven National Laboratory.

Bazant, Z.P. and Kaplan, M.F., 1996, Concrete at High Temperatures: Material Properties and Mathematical Models, Longman, Great Britain.

Dusseault, M.B., Bruno, M.S, and Barrera, J., 1998, Casing Shear: Causes, Cases, Cures, SPE 48864.

Fredrich, J.T., Arquello, J.G., Thorne, B.J. and Wawersik, W.R., 1996, Three-Dimensional Geomechanical Simulation of Reservoir Compaction and Implications for Well Failures in the Belridge Diatomite, SPE 36698, pp. 195-210.

Hilbert, L.B., Gwinn, R.L., Monorey, T.A. and Deitrick, G.L., 1999, Field-Scale and Wellbore Modeling of Compaction-Induced Casing Failures, SPE Drilling & Completion, V. 14(2), pp. 92-101.

Knudsen, S.D., Sattler, A.R. and Staller, G.E., 1999, The Development and Testing of a High Temperature Bridge Plug for Geothermal Casing Remediation, Geothermal Resources Council Transactions, Vol. 23, pp. 159-163.

Marikunte, S., Aldea, C. and Shah, S.P., 1997, Durability of Glass Fiber Reinforced Cement Composites, Advanced Cement Based Materials, V. 5, pp. 100-108

Mossop, A., Murray, M., Owen, S. and Segall, P., 1997, Subsidence at The Geysers Geothermal Field: Results and Simple Models, Proceedings 22nd Workshop on Geothermal Reservoir Engineering, Stanford University, pp. 377-382.

Wagg, B., Xie, J. and Solanki, S., 1999, Evaluating Casing Deformation Mechanisms in Primary Heavy Oil Production, SPE 54116, pp. 257-262.

FIGURES

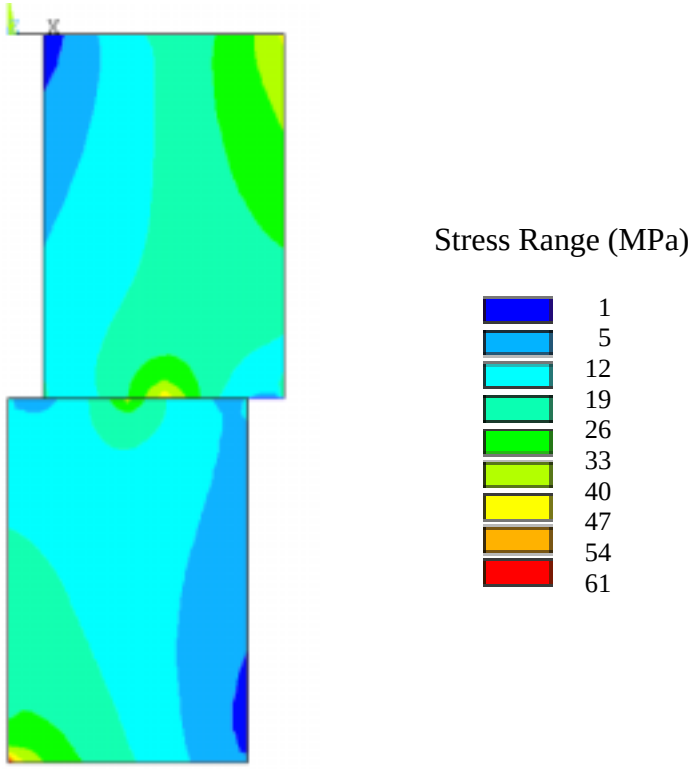

Figure 1. Principal Stresses due to Formation Movement. [return to text]

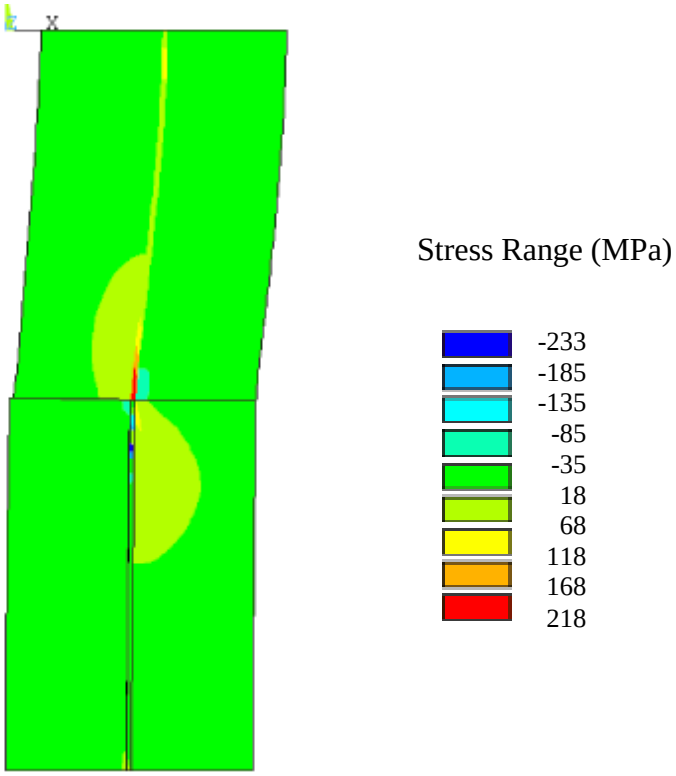

Figure 2. Shear Stress Distribution due to Formation Movement. [return to text]

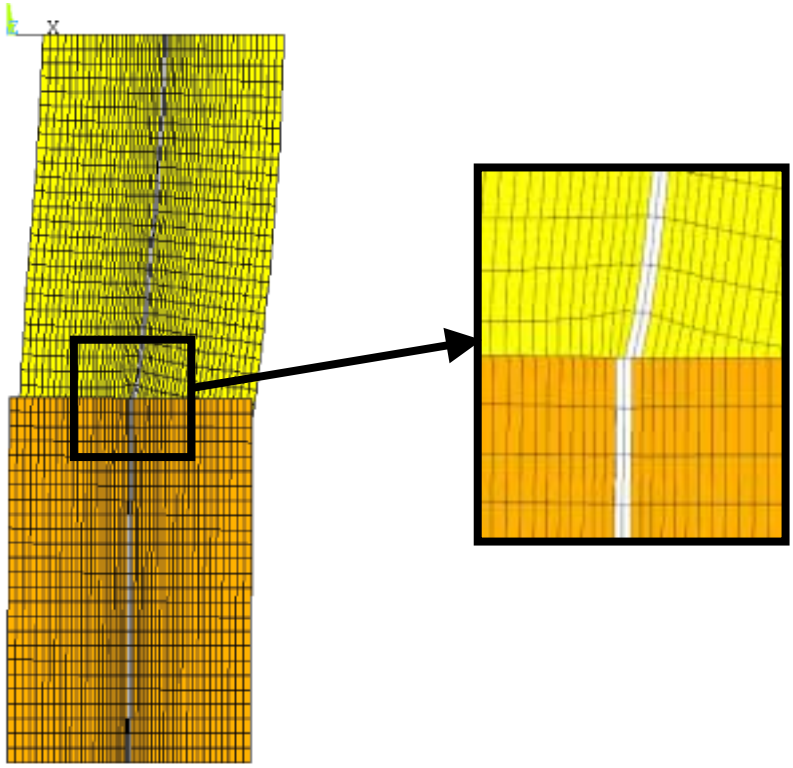

Figure 3. Deformations due to Shearing between Formation Layers. [return to text]

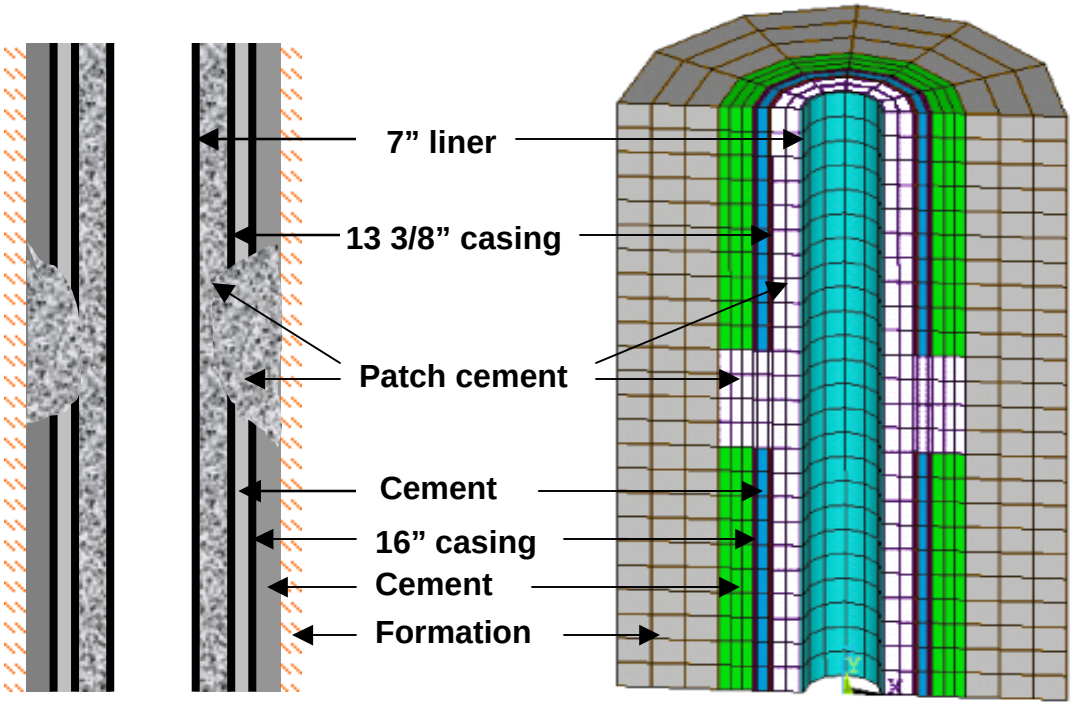

(a) (b)

Figure 4. Cement Patch Configuration (a) [return to text] and associated Finite Element Model (b). [return to text] [return to text2]

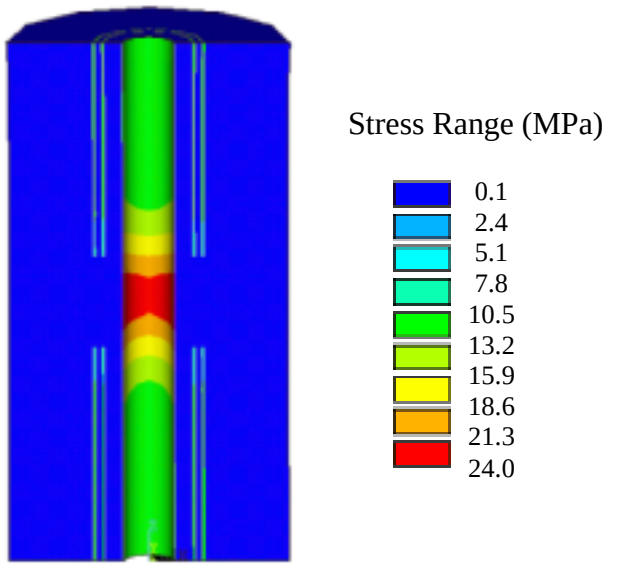

(a)

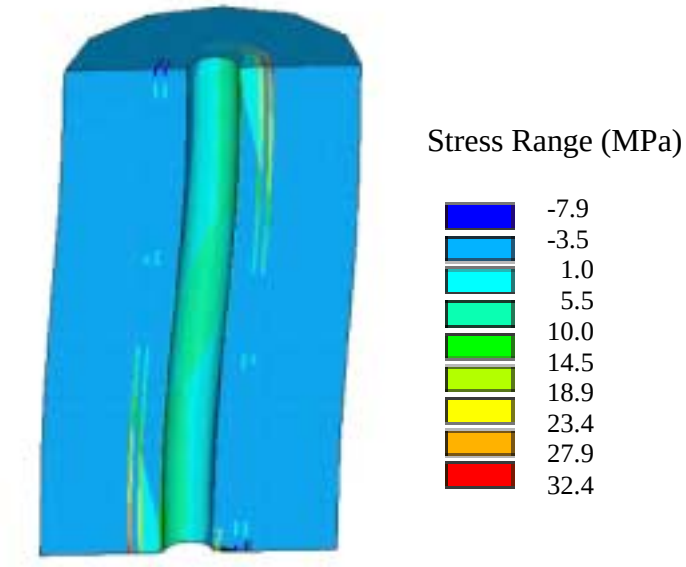

(b)

Figure 5. Stress Distribution due to Axial (a) and Shear (b) Deformation Mechanisms. [return to text]